PAPER • OPEN ACCESS

The flow dynamics behind a flexible finite cylinder as a flexible agitator

To cite this article: T H Yong *et al* 2017 *IOP Conf. Ser.: Mater. Sci. Eng.* **206** 012033

View the article online for updates and enhancements.

The flow dynamics behind a flexible finite cylinder as a flexible agitator

T H Yong[1], H B Chan[2], S S Dol[2], S K Wee[2] and P Kumar[3]

[1]Department of Mechanical Engineering, Curtin University Malaysia
[2]Department of Petroleum Engineering, Curtin University Malaysia
[3]Department of Chemical Engineering, Curtin University Malaysia

Email: wee.siaw.khur@curtin.edu.my

Abstract. This paper investigates the flow dynamics behind a flexible finite cylinder in a single-phase flow using a water tunnel. The cylinder was individually submerged in water at Re_D = 4000, 6000 and 8000. The cylinder investigated has a *AR* = 10 and 16 and is made of EVA in order to achieve the lower stiffness for flexibility. A same *AR* of its aluminium rigid cylinder was investigated to serve as a benchmark to the flow dynamics behind a flexible cylinder. The results the downwash that hinders the transportation of vortices to the downstream was diminished. As a direct consequence of this phenomenon, the turbulence production has seen significant improvement for flexible finite cylinder.

1. Introduction

As a common passive turbulence enhancement method, a rigid cantilever is a very popular candidate to generate turbulence in the wake as it is well-known that flow separates when in contact with bluff body object. The study of flow dynamics behind a rigid cantilever shows highly complicated and three-dimensional flow around the free end. Regular Kármán vortices are supressed near the free end by tip effects but with a good cause as these tip vortices generated have more turbulent energy than the regular Kármán vortices [1]. Rostamy et al. [2] found a higher turbulence intensity and Reynolds stress at the free end. Apart from that, the downwash phenomenon associated with the rigid cantilever draws the fluid downwards to the ground instead of downstream, making most of the high kinetic energy content vortices impinge in the near wake, unable to travel downstream to a greater distance [3]. There have been consistent findings on the flow dynamics behind a rigid cantilever [4-7]. However, there are very little studies reporting on flexible cantilever. The only notable investigation was by Govardhan and Williamson [8] who reported that the Reynolds stress of an elastically-mounted rigid cylinder do increase significantly than that of a rigid cylinder.

In this study, flexibility is introduced into a finite cylinder (hereby refers as 'cylinder') by utilising low stiffness material (*i.e.* ethylene vinyl acetate). The cylinder's flexibility allows the cylinder to oscillate due to the alternating lift force resulted from vortex shedding. It is expected that the oscillating motion of the flexible cylinder alters the fluid dynamics hence generating stronger turbulence level than the rigid (static) cylinder. This study investigates the turbulence enhancement achieved by flexible cylinder by comparing the turbulence production between the rigid and flexible cylinders under the exact same flow condition.

2. Experimental Apparatus and Procedure

2.1. Water Tunnel and Test Models

A circulating open channel water tunnel with a test section of 200 mm x 200 mm in cross section and 750 mm in length was used. Figure 1(a) shows the rigid aluminium test cylinder of $AR = 10$ with a diameter of d = 13 mm and figure 1(b) shows identical cylinder but with $AR = 16$ and a diameter of d = 11 mm. The flexible cylinder in Figure 1(c) is made of ethylene vinyl acetate, EVA and has a diameter of d = 11 mm for both $AR = 10$ and 16. All cylinder has a flat and sharp edge at its free end.
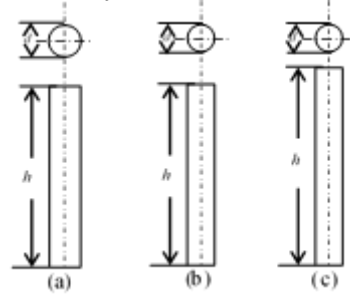

Figure 1. The cylinder models used in this study.

2.2. Experimental set-up

The experimental set-up within the test section is illustrated in Figure 2. A polished smooth surface end plate with 30˚ chamfer on the leading edge was employed to enhance the development of zero pressure gradient boundary layer. This design was also employed by Park and Lee [4] in their experimental work to investigate the free end effects on the near wake flow structure behind a finite circular cylinder. The origin is set at the centre of the cylinder placed perpendicularly to the flow on the end plate at 350mm distance from the leading edge to ensure the boundary layer was fully developed.

Measurements in the near wake (x-z plane) of the cylinder was measured over a 5 mm uniform grid at the top 5D span of the cylinder at streamwise location of x/D = 1 to x/D = 5. At the span below 5D, the measurement point in the wall-normal direction (z plane) increased to a 10 mm uniform grid until 10 mm from the ground. A more refined measurement points was given from the free end to 5D span of the cylinder because tip effects are generally extended up to 3D to 4D from the free end [4, 6, 9]. The cylinder was partially immersed in the boundary layer on the ground plane rating at most of δ/H = 0.43. The blockage ratio was at most 4.8% and no correction was made. The Reynolds number based on the cylinder diameter is $Re_D = 4 \times 10^3, 6 \times 10^3, 8 \times 10^3$.
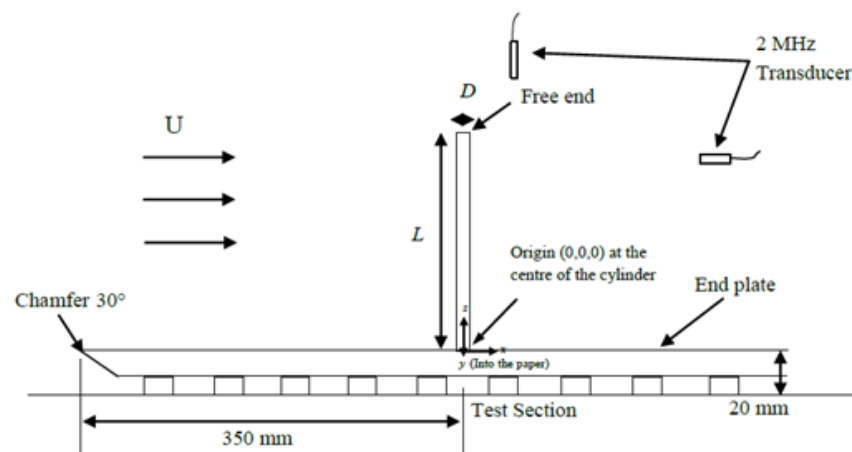

Figure 2. Schematic diagram of experimental set-up in the water tunnel

2.3. Ultrasonic Velocity Profiler
Ultrasonic Velocity Profiler, UVP manufactured by MET-FLOW is used for the measurements of time-averaged flow fields in the wakes. A UVP is a non-intrusive equipment that measures velocity as a function of both space and time in a one-dimensional Eulerian frame. When combined with two or more probes, it can measure a two or three-dimensional flow [10].   The UVP was mounted perpendicular to each other as shown in Figure 2 in the wake behind the cylinder. The horizontal probe was always positioned in a distance 8D downstream the cylinder with reference to the vertical probe to avoid interference in the near wake. Time-averaged streamwise (x-plane) and wall-normal (z-plane) velocity flow fields were measured. The measurement was done at a sampling rate of 100Hz. A total of 4096 profiles were taken for each velocity component.

3. Experimental Results and Discussion
The u- and w- components velocity profiles of AR=10 and AR=16 cases are shown in Figure 3 and 4 respectively.

3.1. Velocity profiles of rigid cylinder in the wake of x-z plane
The velocity components (u/U, w/U) of rigid cylinder at 5D downstream of the cylinder are presented. With reference to the u component, there is a very steep velocity gradient at the region near the free end for both AR. These changes are caused by the tip effects where the tip vortex plays a role. In general, the strong influence of tip effects can be seen taking effective to approximately 3D from the free end. The same phenomenon is consistently reported by Rostamy et al. [2]; Park & Lee [4]; Okamoto & Yagita [6]; Roh & Park [9].

Below the steep velocity gradient (indicated by double-dot dashed arrow) is a strong velocity defect that has a rather consistent profile where regular Kármán vortex is likely to exist. The strong velocity defect can serve as a 'body' of the wake region. The velocity defect happens due to the presence of vortical motion in the flow field which extract the energy from the mean flow, resulting in the lower fluid velocity [11]. Therefore, the wake region is approximately 3D shorter than the free end. When examined together with the w component, the higher value of localized negative w-component velocity at approximately x/D < 3 shows that the flow is brought downwards instead of downstream. It is a common phenomenon called downwash. The vortices generated are brought toward the floor immediately since they follow the path of the mean flow. Since the motion of vortex is hindered at near wake, it causes the region of augmented turbulence region effective in the very near wake. The variation in Re contributes minor influence to the velocity profiles behind a rigid cylinder.

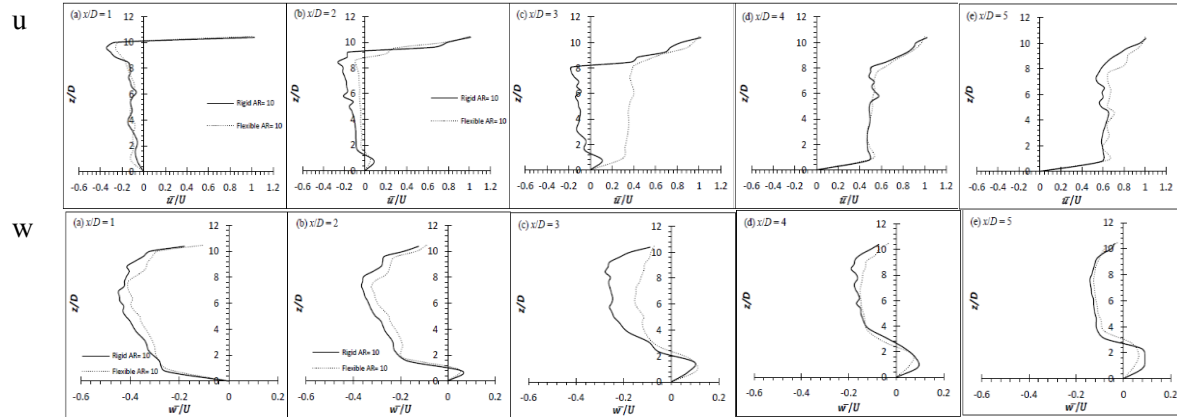*3.2. Velocity profiles of flexible cylinder in the wake of x-z plane*
To the best of author's knowledge, the velocity profiles of passively-oscillating flexible cylinder are uncommon, if not none. It is worth noting that since the flexible cylinder was deflecting during measurements, measurements in x/D ≤ 3 were hindered by the deflected cylinder and could not be measured (depending on the degree of deflection). However, the earliest available measurements were put into comparison with rigid cylinder at x/D = 1 as it is the nearest position to the free end.

In general, as can be seen with the cylinders that deflect (AR = 16 at Re 4000, 6000 and 8000), the most noticeable observation is that the localized w-component velocity is weaker in the case of flexible cylinder. The lower value of localized w component as opposed to u component in the very near wake signifies that the influence of downwash is diminished. As a result, the vortices generated can be transported downstream instead of downwards. This observation suggests that the turbulence energy carried by the vortices can be delivered to downstream more effectively, resulting an increasing turbulence production at downstream. This shall be seen from the turbulence production in the under section.

Re=4000

u

w

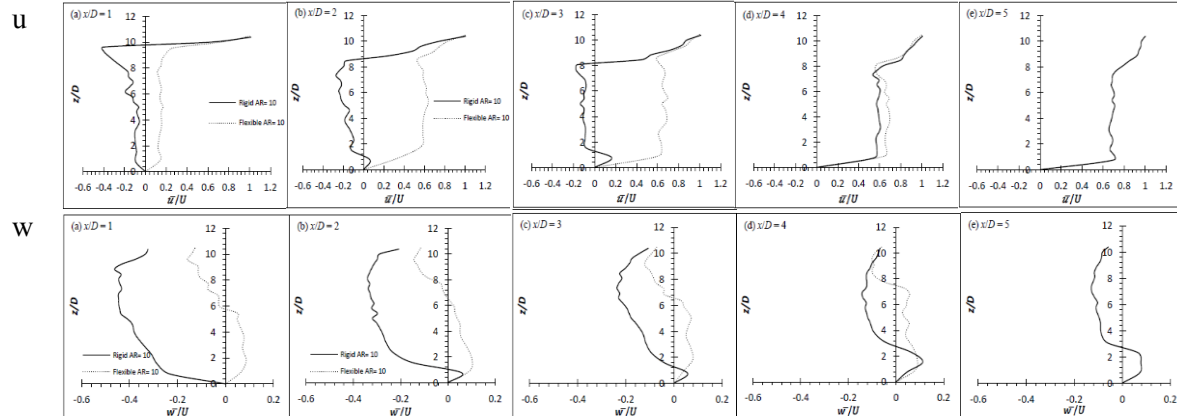

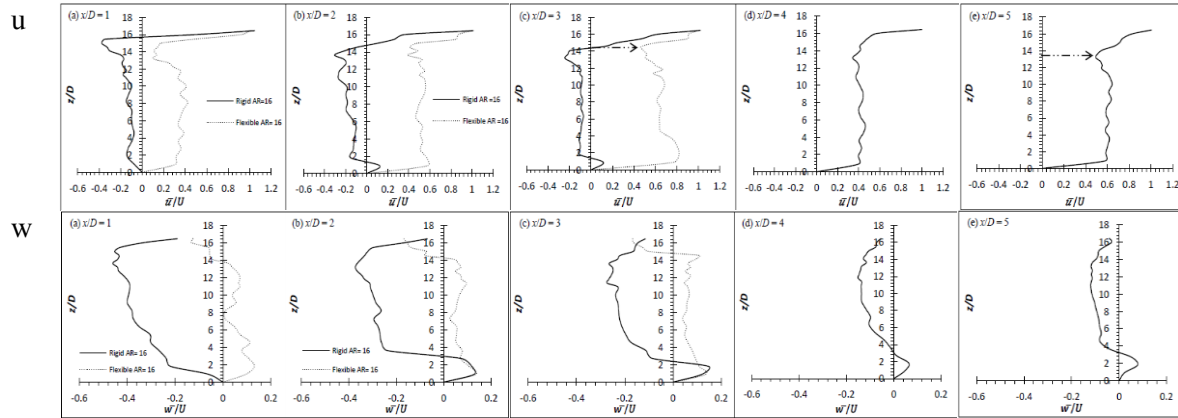Re=6000

u
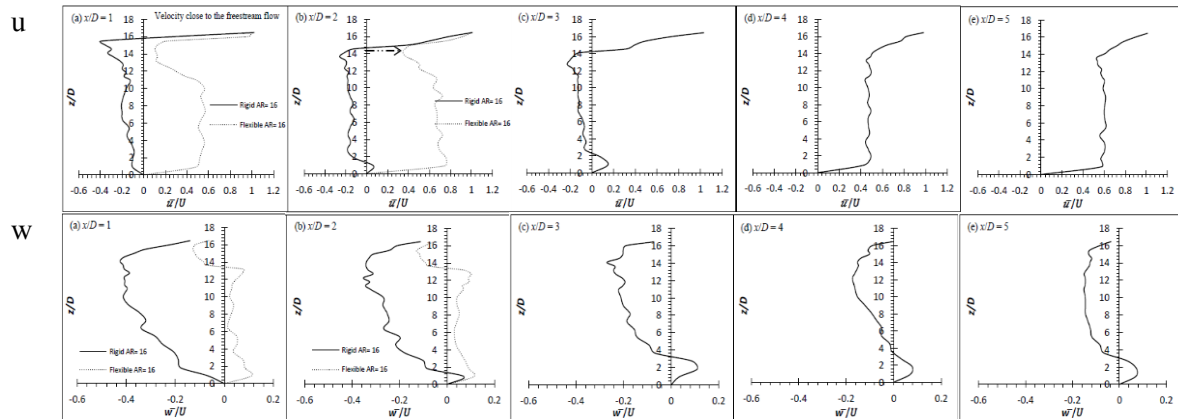

w

Re=8000

u

w
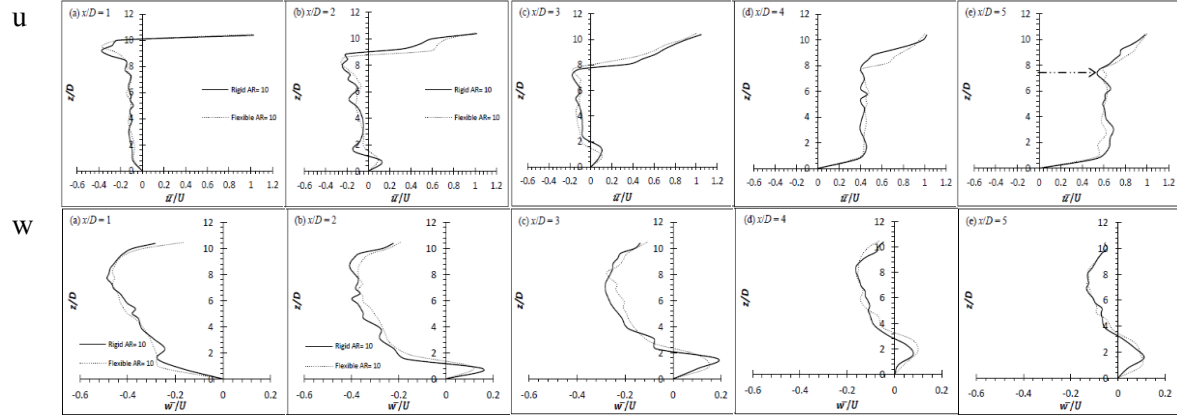
Figure 3. Time-averaged u and w component velocity profile of rigid and flexible cylinder of AR=10 at Re=4000, 6000 and 8000.
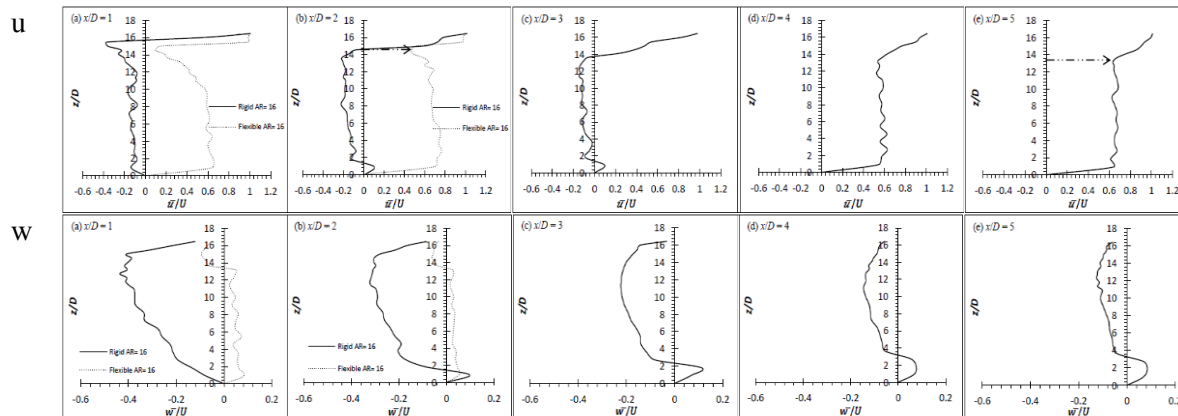
Re=4000

Re=6000

Re=8000

Figure 4. Time-averaged u and w component velocity profile of rigid and flexible cylinder of AR=16 at Re=4000, 6000 and 8000.

3.3. Turbulence production of rigid and flexible cylinders in the x-z plane

As mentioned earlier, the turbulence production between rigid and flexible case are compared to identify the greater turbulence enhancement achieved by flexible cylinder. With reference to this, the evolution of turbulent kinetic energy production is investigated in this section. The production term, (labelled as **P** for convenience) which is part of the kinetic energy budget equation, analyses the amount of energy that is contributed to the turbulence formation from the mean flow. The **P** term that is being evaluated here is:

$$\boldsymbol{P} = -[(u'\,u'\,)\cdot\partial u/\partial x+(u'\,w'\,)\cdot\partial U/\partial z+(u'\,w'\,)\cdot\partial w/\partial x+(w'\,w'\,)\cdot\partial w/\partial z] \tag{1}$$

The *P* of rigid case is as shown in Figure 5; flexible case is as shown in Figure 6.
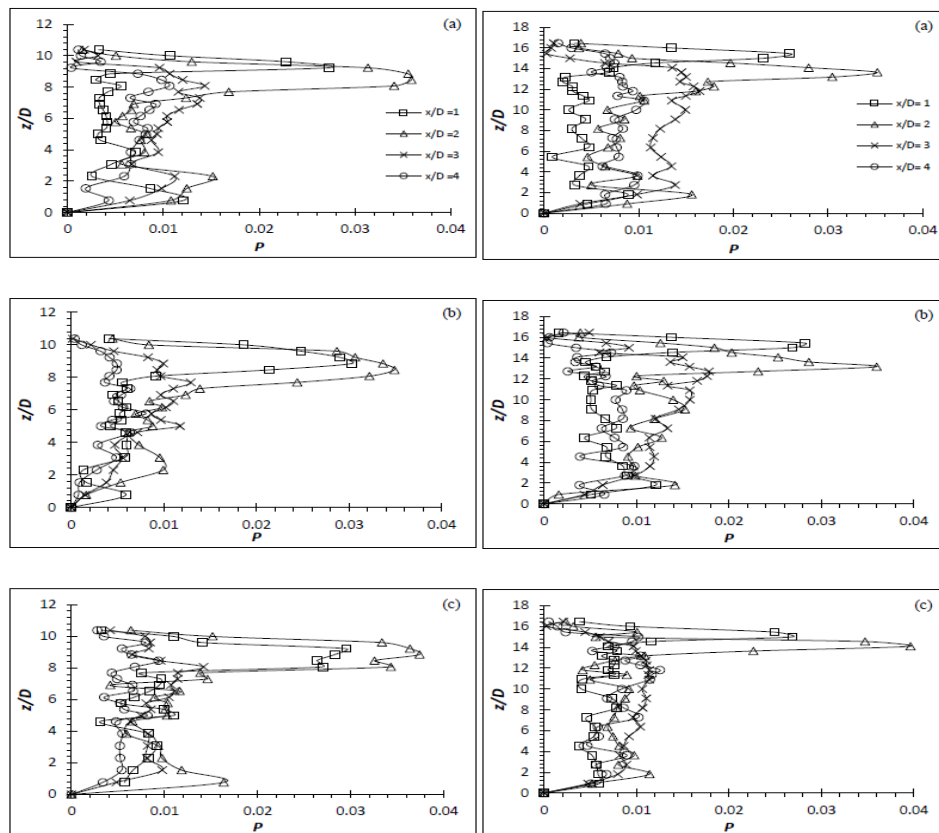

Figure 5. Production term for rigid cylinder of (left) AR=10 and (right) AR=16 at Re= (a) 4000, (b) 6000 and (c) 8000.

Based on the *P* behind the rigid cylinder as shown in Figure 5, it is observed that the *P* term varies at different *z*-location. The greatest *P*, *i.e.* ~0.036m^2/s^3, is located approximately 2D below the free end of the cylinder and is impinged in near the wake, x/D ≤ 2. This is in good agreement with the mean flow velocity profiles (Figure 3 and 4) where the downwash transports most of the vortices downwards (*i.e.* right behind the cylinder). In other words, the vortices are temporally trapped in the near wake (x/D<2) due to downwash resulting the maximum *P* to occur in near wake region.

The *P* term for the flexible cylinder on the other hand (Figure 6), do see significant increase in value due to the effectiveness of VIV in increasing the strength of vortices shed [12]. The maximum increment achieved by flexible cylinder is 127% (2.27 times greater), which can be seen at x/D=4 of the AR=16 flexible cylinder. These elevated *P* values clearly show the stronger turbulence level behind a flexible cylinder than that of a rigid cylinder. Hence, proving that a flexible cylinder is indeed a better turbulence generator.

Besides, this is also an expected result as the previous finding (*i.e.* vortices are transported downstream instead of downwards due to the diminishing of downwash) has suggested that the energy carried by the vortices generated from the flexible cylinder can be transported to the downstream directly and more effectively. The fact that the *P* term is seen expanding to downstream further than that of rigid cylinder (*i.e.* maximum happened at x/D=4 instead of 2 as shown in rigid case) signifying the previous explanation is correct and the augmented turbulence level is indeed covering a greater region as discussed previously.
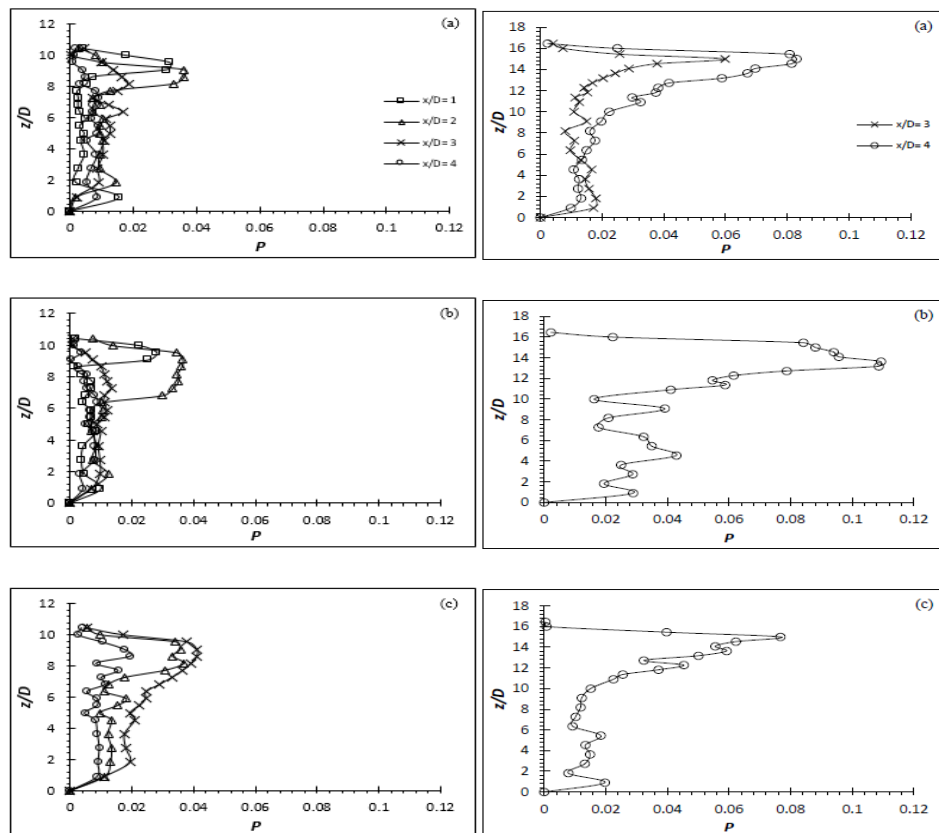
Figure 6. Production term for flexible cylinder of (left) AR=10 and (right) AR=16 at Re= (a) 4000, (b) 6000 and (c) 8000.

4. Conclusion

The flow dynamics behind flexible and rigid cylinder is experimentally studied and compared in this research. The flexible cylinder has shown to be a promising alternative to conventional rigid cylinder as agitator. Based on the current turbulence production (**P** term) analysis, the flexible cylinder can generate turbulence that is, at maximum 2.27 times, of the amount generated by the rigid cylinder under the same flow condition. This clearly shows that the turbulence production of the flexible cylinder is significantly greater than that of the rigid cylinder. Based on the current analysis, it is found that one of the contributors of such elevation is due to the weakening of downwash behind the flexible cylinder as shown from the u- and w-component velocity profiles. As a result, the flow can be transported downstream more effectively, so are the vortices generated as they generally follow the path of the mean flow. Subsequently, the turbulence production, **P** shows a greater value at the downstream of the flexible cylinder, signifying stronger turbulence.

References
[1]   Sumner D 2013 Flow above the free end of a surface-mounted finite-height circular cylinder: a review *J.l of Fluids and Struct.* **43** 41-63
[2]   Rostamy N, Sumner D, Nergstrom DJ, and Bugg JD 2012 Local flow field of a surface-mounted finite circular cylinder *J. of Fluids and Struct.* **34** 105-22
[3]   Kawamura T, Hiwada M, Hibino T, Mabuchi I and Kumada M 1984 Flow around a finite

circular cylinder on a flat plate: cylinder height greater than turbulent boundary layer thickness *Bulletin of JSME* **27**(232) 2142-51

[4]   Park CW and Lee SJ 2000 Free end effects on the near wake flow structure behind a finite circular cylinder *J. of Wind Eng. and Ind. Aerodynamics* **88**(2) 231-46

[5]   Park CW and Lee SJ 2004 Effects of free-end corner shape on flow structure around a finite cylinder *J. of Fluids and Struct.* **19**(2) 141-58

[6]   Okamoto T and Yagita M 1973 The experimental investigation on the flow past a circular cylinder of finite length placed normal to the plane surface in a uniform stream *Bulletin of JSME* 19(**95**) 805-14

[7]   Sumner D, Heseltine JL, and Dansereau OJP 2004 Wake structure of a finite circular cylinder of small aspect ratio. *Exp. in Fluids* **17**(5) 720-30

[8]   Govardhan R and Williamson CHK 2001 Mean and fluctuating velocity field in the wake of a freely-vibrating cylinder *J. of Fluids and Struct.* **15**(3) 489-501

[9]   Roh S and Park S 2003 Vortical flow over the free end surface of a finite circular cylinder mounted on a flat plate *Exp. in Fluids* **34**(1) 63-67

[10]   Yokoyama K, Kashiwaguma N, Okubo T and Takeda Y 2004 Flow measurement in an open channel by UVP *proceedings ISUD* **4** 201-10

[11]   Chan HB, Yong TH, Kumar P, Wee SK and Dol SS 2016 The numerical investigation on the effects of aspect ratio and cross-sectional shape on the wake structure behind a cantilever *ARPN J. of Eng. and App. Sci.* **11**(16) 9926-32

[12]   Thulukkanam K 2013 *Heat exchanger design handbook* CPC Press